Journal of Porous Materials (2023) 30:1789–1795
https://doi.org/10.1007/s10934-023-01463-x

Effects of Zr, Al, and mordenite on Pt-MCM-48 catalyst in n-heptane isomerization: preparation, characterization and catalytic performance

Z. Ghaderi[1] · M. H. Peyrovi[1] · N. Parsafard[2]

Accepted: 18 April 2023 / Published online: 2 May 2023

Abstract
Herein, platinum-loaded MCM-48-Mordenite, Al-MCM-48, Al-MCM-48-Mordenite, Zr-MCM-48, and Zr-MCM-48-Mordenite catalysts were synthesized and studied for the isomerization reaction of n-heptane at four different temperatures. XRD, XRF, FT-IR, UV-Vis DRS, NH_3-TPD, TG/DTA and BET analysis were used to characterize the structural characterizationand acid distribution of these catalysts. The Pt/Mordenite catalyst showed higher hydrogenation and cracking activity, while the hybrid catalysts showed better isomerization selectivity. The Pt/Al-MCM-48-Mordenite catalyst showed the best catalytic behavior at 200 °C with a suitable n-heptane conversion (78.8%) and the highest isomer selectivity (81.9%). The maximum isomerization selectivity as well as the maximum yield of multi-branched isomers are probably not only due to the suitable acidity and the large pores, but also to the higher metal dispersion. This result shows that the Pt/Al-MCM-48-Mordenite catalyst can be a hopeful candidate for good n-heptane isomerization catalysts.

Keywords n-Heptane isomerization · Catalyst · Catalytic performance · Pt/Al-MCM-48-mordenite

1 Introduction

Environmental laws limit the content of aromatics, benzene and other harmful fuel compounds that affect the quality of gasoline. A suitable alternative to aromatics are branched paraffins with a high octane number. Accordingly, isomerization of paraffins has been introduced as an important reaction for the production of high quality gasoline [1–4]. This process is carried out at low temperatures to prevent cracking and aromatization. The rate of this reaction is slow, and so the catalyst used must be very active. The use of strongly acidic catalysts lowers the reaction temperature and increases the tendency to form branched alkanes with high octane numbers.

In order to produce acid catalysts that achieve the best efficiency in the isomerization of paraffins, modification treatment with various metals such as Co [5], Mn [6], Fe [7], Zr [8], Ti [9, 10] and Al [11] has already been investigated. The excellent ion exchange capacity makes zirconia a good promoter or support in catalytic processes.

In 2020, Parsafard et al. prepared collections of Pt–Cr/Zr(x)-HMS catalysts with different molar ratios of Cr/Zr and used them as solid acid catalysts for the isomerization of n-heptane. The best selectivity for isomeric products was observed at Cr/Zr = 30 [12].

The mesoporous composite catalysts, when used in the isomerization reaction, can effectively increase the diffusion rate of multi-branched hydrocarbons due to their mesoporous structure, allowing them to pass rapidly through the zeolite micropore channels and reducing side reactions such as cracking [13]. The mass transfer yield in 3D cubic mesopores such as MCM-48 and KIT-6 is higher than that in 2D straight channels, which is due to the highly interpenetrating and cross-linked 3D mesostructure [14]. In 2021, Ghaderi et al. show that the Pt/MCM-48-HZSM-5 catalyst exhibits good selectivity for multi-branched isomers and also demonstrates catalytic stability during the isomerization reaction [15].

✉ N. Parsafard
n-parsafard@kub.ac.ir

[1] Department of Physical and Computational Chemistry, Faculty of Chemistry Science and Petroleum, Shahid Beheshti University, Tehran 1983963113, Iran

[2] Department of Applied Chemistry, Kosar University of Bojnord, Bojnord, North Khorasan, Iran

It is well known that the acidity and porosity of zeolite materials significantly affect the catalytic performance. Although platinum (Pt) metal supported on zeolites inhibits the coke formation, the catalytic conversion and selectivity to iso-products are still low [16, 17].

The researchers investigated the effect of adding different zeolites such as beta, mordenite or HZSM-5 to Pt/AlSBA-15 catalysts. The results show that the composites perform better in isomerization compared to Pt/AlSBA-15 [18]. In another study, the influence of the ratio of AlSBA-15 to zeolite on the physicochemical properties was investigated. In this work, micro-mesoporous materials with different amounts of beta zeolite were used as supports for platinum catalysts for the hydroisomerization of n-heptane. The results show that the introduction of zeolite into AlSBA-15 in the synthesis step affects the acidity of the composite materials. Both the strength of the acid sites and the overall acidity depended on the ratio of AlSBA-15 to zeolite. Catalysts with 14 and 25 wt% zeolite gave the highest yield of high octane isoheptane products. The most promising Pt/AlSBA-15 + zeolite catalysts (i.e. with 14 and 25 wt% beta) allow allow an improvement of the research octane number from 0 to 65–70 points [19].

Mordenite zeolite is used for many catalytic reactions such as alkylation, isomerization and dehydrogenation due to its uniform, controlled chemistry, flexible framework and large internal surface area [20]. This zeolite has two types of channels: larger and smaller channels. This zeolite is also a very strong acid catalyst [21].

In the present study, a Pt/MCM-48 catalyst modified with zirconium, aluminium, and mordenite zeolite was investigated and used as a solid acid catalyst in the reaction to produce multi-branched compounds from n-heptane. The parameters such as activity, selectivity for different products, stability, coke deposition and RON (research octane number) were discussed in the temperature range of 200–350 °C.

2 Experimental

2.1 Catalyst preparation

Mordenite zeolite was prepared according to the procedures described in the literature [22, 23]. 4.75 g sodium hydroxide was dissolved in 10 ml water, then 3.57 g sodium aluminate was added and the mixture was stirred until dissolved. Finally, 161.25 ml of water and 24.55 g of SiO_2 were added and the mixture was stirred for 48 h. The mixture was then dissolved. The molar composition of this mixture solution was 6 Na_2O:1 Al_2O_3:30 SiO_2:780 H_2O. The gel obtained was placed in a Teflon-lined steel autoclave and kept at 180 °C for 24 h for crystallization. The product was filtered, washed and dried for 10 h at 100 °C. The sample was ion-exchanged with a NH_4NO_3 solution (1 M) for 1 h at 60 °C. This procedure was repeated three times and then the powder obtained was calcined at 500 °C.

The MCM-48-Mordenite was synthesized according to the method described in [15]. 2.4 g of cetrimonium bromide (CTAB) was dissolved in 50 ml of water, and then 0.5 g of mordenite was added to the mixture. Then, 12 ml of ammonia (32 wt%) and 50 ml of ethanol were added to the solution and stirred for 15 min. Then, 3.4 g of tetraethyl orthosilicate (TEOS) was added to the solution. The mixture was stirred for 2 h at room temperature. The resulting mixture was kept at room temperature for 24 h for crystallization. The solid obtained was recovered by filtration and dried in air. Finally, the sample was calcined at 500 °C for 4 h.

For the preparation of Zr-MCM-48 and Al-MCM-48, 0.18 g of zirconyl nitrate ($ZrO(NO_3)_2 \cdot 6H_2O$) or 0.28 g of aluminium nitrate ($Al(NO_3)_3 \cdot 9H_2O$) were added to the solution instead of the mordenite. This method was used for the synthesis of the catalyst with Si/Zr and Si/Al = 20. In the preparation of Zr-MCM-48-Mordenite and Al-MCM-48-Mordenite, 0.5 g of mordenite was also added after the addition of zirconyl nitrate or aluminium nitrate.

In addition, catalysts containing platinum (0.6 wt%) were also prepared by impregnating the support with a suitable concentration of hexachloroplatinic acid. The catalysts were filtered and dried overnight at 110 °C. Subsequently, these solid samples were calcined in air at 300 °C for 4 h.

2.2 Characterization tests

Powder X-ray diffraction patterns (XRD), Fourier transform infrared spectroscopy (FTIR), X-ray fluorescence (XRF), ultraviolet-visible diffuse reflectance spectra (UV-Vis DRS), nitrogen adsorption isotherms, and temperature-programmed desorption of ammonia (NH_3-TPD) were performed using an X-PERT diffractometer, a BOMEM FT-IR spectrophotometer, XRF-8410 Rh, a Shimadzu UV-2100 spectrophotometer, a ASAP-2010 micromeritics instrument and a TPD/TPR analyzer (2900 micromeritics) instrument, respectively.

Thermal analysis (TG/DTA) was performed in air at a heating rate of 10 °C min^{-1} using a Bahr STA-503 instrument.

The specific analytical conditions are given in our previous work [12, 15] for each characterization method.

2.3 Catalytic evaluation

At the beginning of the experiment, 0.2 g of catalyst was loaded into a continuous fixed bed reactor. The reaction temperature for all samples started at from 200 °C and increased to 250, 300 and 350 °C. The catalysts were reduced in a H_2 gas stream (40 ml/min) at 400 °C (2 h) before each experiment. The n-heptane (n-C_7) was fed into the reactor with a

syringe pump at a flow rate of 2 ml/h and mixed with the H_2 stream. The efficiency of the calcined catalysts was tested after 1 h in the stream at each temperature and atmospheric pressure. The efficiency of all the catalysts prepared was also tested at 300 °C for 6 h in the stream to determine the amount of coke deposition. Analysis of the reactor products was carried out at GC-FID using an Agilent Technologies 7890 A.

The catalytic activity is expressed by the n-C_7 conversion calculated by the following Equation.

$$\text{Conv. (\%)} = \text{the percentage of the total amount of n} - C_7 \text{ converted} \quad (1)$$

In addition, the following equation was used to calculate the selectivity for different products:

$$S_x(\%) = \frac{\text{n} - C_7 \text{ converted to a given product}}{\text{total amount of n} - C_7 \text{ converted}} \times 100 \quad (2)$$

3 Results and discussion

3.1 Catalysts characterization

Figure 1 shows the XRD patterns of the prepared catalysts. The typical peaks of MCM-48 are seen at 2θ = 2.9°, which is due to the d_{211} diffraction of the cubic phase of MCM-48, and the peak at 2θ = 3.4° shows the d_{220} reflection [24, 25]. The mordenite structure shows sharp peaks in the range 9–36°, which correspond to the reflections of the mordenite zeolite. The diffraction peaks at 9.77°, 13.46°, 19.62°, 22.20°, 23.17°, 25.64°, 26.25°, 27.67°, 27.85°, 30.89° and 35.61° show that the mordenite was successfully synthesized [26, 27]. Meanwhile, the XRD patterns do not show signals of zirconia, platinum and aluminium metals, which is probably due to the homogeneous dispersion of these metallic phases within the synthesized catalysts. However, the presence of these metals was verified by an XRF test.

The FTIR spectra of the synthesized catalysts are shown in Fig. 2. The FTIR spectra of MCM-48-Mordenite and other composites show bands at 1639 and 3400 cm^{-1}, indicating the presence of physisorbed water. The characterization bands of MCM-48 are seen at 1234 and 1080 cm^{-1}, which are assigned to v_{as}(Si-O-Si). Also, the absorption bands at 460 cm^{-1} and 810 cm^{-1} usually belong to δ(Si–O–Si) and v_s(Si–O–Si) [28]. The FT-IR spectra of mordenite zeolite show the bands at 1080 cm^{-1} (asymmetric stretching vibration of Si–O bond), 810 cm^{-1} (symmetric stretching vibration of Al–O bond), 580 cm^{-1} (vibration of five-membered rings) and 450 cm^{-1} (T–O bending) [26]. Furthermore, no absorption band corresponding to the aluminium and zirconium phase was found in the FTIR spectra, which also confirms a good dispersion of aluminium and zirconium.

The UV-vis diffuse reflectance spectra of the samples are shown in Fig. 3. This analysis was used to distinguish the chemical structure of Pt. The band near 250 nm is a charge transfer band (CT) (oxygen to metal) and is seen in all spectra. Also, the weak shoulder at above 350 nm must be due to a d-d transition band of Pt^{2+} species [29]. The observed shifts in the intensities of these peaks may be due to the different interaction strength of the species and their population on the supports.

The acid distributions on the surface of the synthesized catalysts are shown in Table 1. In the tables, the synthesized catalysts are referred to as M: Mordenite, MM: MCM-48-Mordenite, ZM:Zr-MCM-48,

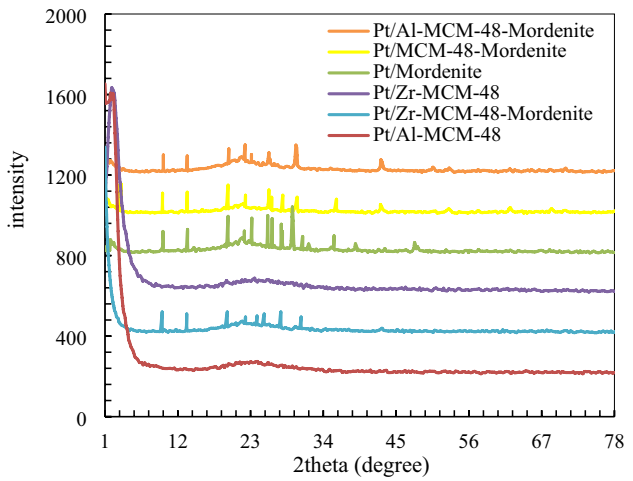

Fig. 1 XRD patterns for the Pt-supported catalysts

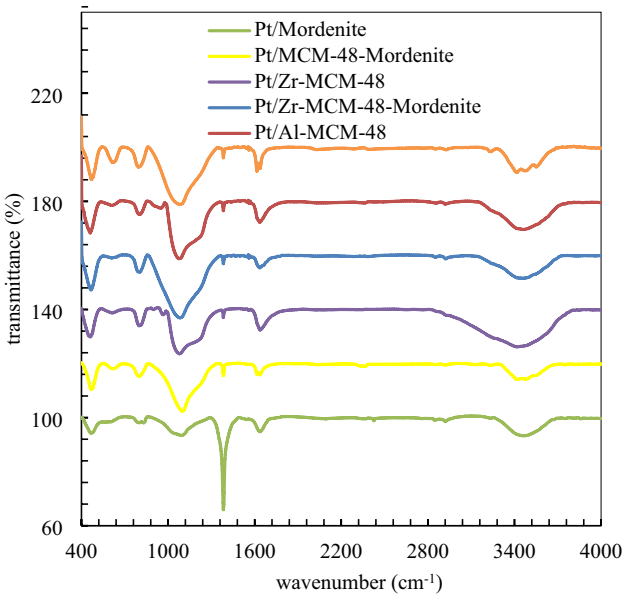

Fig. 2 The FT-IR spectra for the Pt-supported catalysts

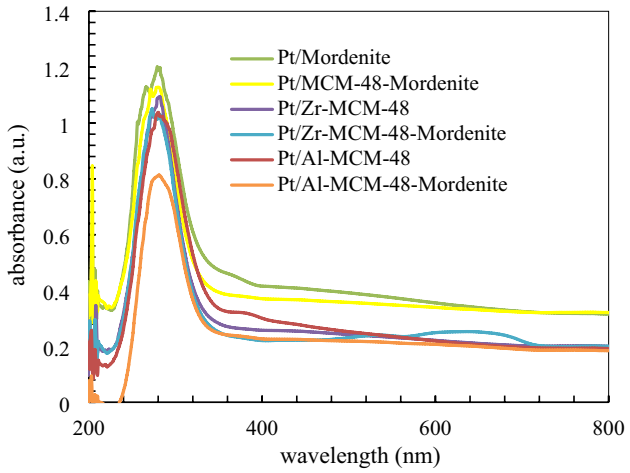

Fig. 3 UV-vis DRS for the synthesized catalysts

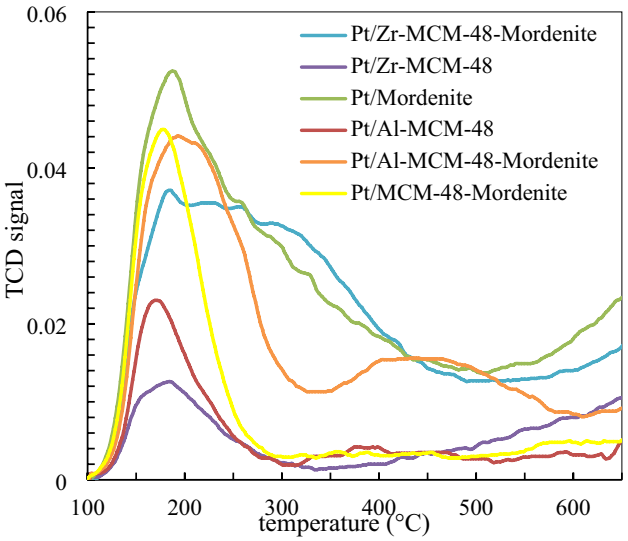

Fig. 4 NH_3-TPD profiles for Pt-supported catalysts

ZMM:Zr-MCM-48-Mordenite, AM:Al-MCM-48, and AMM:Al-MCM-48-Mordenite.

Figure 4 also shows the acid site distributions for the calcined catalysts determined by NH_3-TPD.

All samples show two desorption peaks in the temperature range 100–650 °C, interpreted as weak and strong acids. The data in Table 1 show that the number of weak acid sites is lower for all catalysts than for mordenite. The amounts of weak acid in these samples range from 57 to ~ 308 mmol g_{cat}^{-1}, and those of strong acid range from 111 to ~ 322 mmol g_{cat}^{-1}.

The density of the total acid sites of the catalysts follows the below order:

Pt/Mordenite > Pt/Al-MCM-48-Mordenite > Pt/Zr-MCM-48-Mordenite > Pt/MCM-48-Mordenite > Pt/Al-MCM-48 > Pt/Zr-MCM-48.

In other words, the strength of the acid sites in the Pt/Al-MCM-48 and Pt/Zr-MCM-48 catalysts increases with the addition of mordenite zeolite.

Figure 5 shows the adsorption/desorption isotherms of all samples. The curves of the samples showed typical Langmuir IV adsorption isotherms (ICPU), indicating that the catalysts have a certain amount of slit-like pores. For comparison, Table 1 summarizes the textural properties of the prepared catalysts (S_{BET}, V_P, and d_P). The results show that the Pt/Al-MCM-48 catalyst has the highest BET surface area (S_{BET}). Moreover, the specific surface area and pore volume of Pt/Al-MCM-48 and Pt/Zr-MCM-48 decrease after composite formation with mordenite. However, the pore diameter decreases. Moreover, Pt/Al-MCM-48-Mordenite has a larger pore diameter (5.3 nm) than other catalysts.

Table 1 Physicochemical properties of the Pt-synthesized catalysts

Catalysts	M	MM	ZM	ZMM	AM	AMM
Acidity (μmol NH_3/g)						
W	307.6	245.6	57.2	283.3	86.1	231.2
S	264.5	120.7	115.8	256.4	110.7	321.7
W + S	572.1	366.3	173.0	539.7	196.8	552.9
S/W	0.9	0.5	2.0	0.9	1.3	1.4
Surface properties						
S_{BET} (m^2/g)	341.1	398.2	458.4	158.8	771.9	378.2
V_p (cm^3/g)	0.28	0.71	0.25	0.16	0.67	0.59
d_p (nm)	3.3	3.4	2.2	4.1	3.5	5.3
Elemental analysis						
Si/Al	9.6	10.5	–	10.2	20.0	32.5
Si/Zr	–	–	18.9	23.3	–	–
Pt%	0.50	0.58	0.52	0.52	0.54	0.60

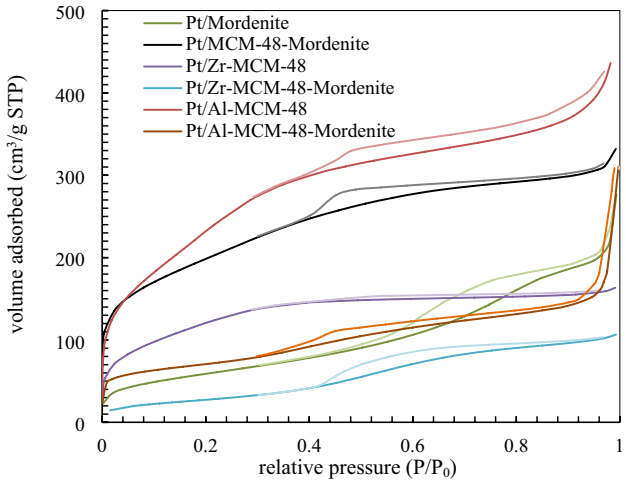

Fig. 5 N_2 adsorption and desorption isotherms for Pt-loaded catalysts

3.2 Catalytic isomerization of n-C_7

The catalytic performance of the Pt-loaded mordenite, MCM-48-Mordenite, Zr-MCM-48, Zr-MCM-48-Mordenite, Al-MCM-48 and Al-MCM-48-Mordenite catalysts was investigated for the n-C_7 isomerization reaction in the range of 200–350 °C. Table 2 shows the catalytic properties of the synthesized catalysts. It can be seen that the n-heptane conversion increases with increasing temperature for all catalysts. The highest n-C_7 conversion, 96.7%, is obtained with the catalyst Pt/Al-MCM-48-Mordenite at 350 °C. It is assumed that the n-heptane conversion of catalysts often depends on the acid strength of the catalysts, as the probability of interaction between the acid sites and the olefinic intermediates increases [30–32].

The density of acidic sites was qualitatively determined by the location of the maximum peak temperature in the profiles of TPD. In addition, the selectivity results for mono-branched (S_{MOB}) and multi-branched (S_{MUB}) isomers and total i-C_7 (S_{i-C7}) were presented in Table 2. These results show that at low reaction temperature, the selectivity for iso-heptanes is high for all catalysts. This is because the isomerization reaction has a thermodynamic limit. In other words, temperature is a limiting factor in this reaction. In the synthesized catalysts, the ratio of MUB isomers to MOB isomers (R) is almost always between 1.0 and 3.0. The selectivity for MUB isomers is higher than for MOB isomers in all catalysts. The selectivity towards the MUB isomers depends on the surface properties of the catalysts, such as the pore volume (V_p) and diameter (d_p). The Pt/Al-MCM-48-Mordenite has a large pore size (5.3 nm). This catalyst with the right pore size allows good diffusion of the MUB

Table 2 Catalytic activity (Conv.%), selectivity (S_x%), coke amount (%) from combustion (C) and TG/DTA (C*), and RON at different reaction temperatures with Pt-synthesized catalysts

Catalyst	T/°C	C	C*	Conv.	S_{MOB}	S_{MUB}	S_{i-C7}	S_C	S_A	S_H	RON
AMM	200			78.8	24.4	57.5	81.9	4.2	0.4	13.9	96.5
	250			86.7	15.2	38.4	53.6	10.7	0.7	34.9	84.6
	300	7.8	8.1	90.1	8.0	16.9	25.0	17.7	0.9	56.3	63.3
	350			96.7	3.2	8.9	12.2	20.3	1.4	66.3	58.5
AM	200			47.8	25.7	42.4	68.1	2.3	0.1	29.5	60.9
	250			50.7	26.3	28.2	54.5	4.2	0.2	41.1	59.6
	300	4.7	4.4	54.8	13.3	15.1	28.4	8.5	0.2	63.0	58.2
	350			64.8	5.1	7.2	12.3	14.0	0.5	73.1	56.3
ZMM	200			65.7	23.0	38.5	61.5	8.0	0.6	29.8	68.4
	250			74.7	21.7	24.6	46.3	12.0	0.9	40.8	64.1
	300	7.2	7.5	81.7	10.0	14.7	24.7	16.3	2.2	57.0	57.6
	350			89.4	3.3	7.8	11.1	19.0	3.2	66.7	52.8
ZM	200			42.7	22.6	35.0	57.6	5.7	0.1	36.5	49.0
	250			46.7	15.0	25.0	40.0	14.1	0.3	45.6	39.0
	300	4.1	3.9	49.6	10.6	16.8	27.4	17.1	0.4	54.5	35.0
	350			55.7	4.2	4.8	9.0	20.3	0.5	70.1	34.5
MM	200			59.8	34.6	42.2	76.8	5.3	0.2	17.7	65.6
	250			67.6	16.6	33.1	49.7	11.9	0.5	37.9	62.3
	300	6.3	6.7	75.8	8.3	15.5	23.8	18.0	1.1	57.1	51.9
	350			81.3	3.9	6.3	10.2	20.2	1.9	67.7	47.3
M	200			71.8	14.3	16.2	30.5	16.5	0.5	52.5	52.3
	250			84.7	8.2	9.0	17.3	20.0	0.6	62.1	51.6
	300	3.4	3.3	91.6	3.6	3.6	7.2	22.1	1.1	69.7	48.8
	350			95.7	0.7	0.8	1.5	23.4	1.2	73.8	46.8

isomers through the pores before they are cracked. Thus, the Pt/Al-MCM-48-Mordenite catalyst has the best selectivity for MUB isomers and the best R-value. MUB isomers are a key product of the isomerization process due to their high octane number and great importance in the oil industry, providing greater fuel resistance to knock or ping during combustion. In Table 2, we have also shown the selectivity of the cracking products (main product: 3-hexyne), aromatization (main product: toluene) and hydrogenolysis (main products: H_2 and CH_4) of n-C_7 as a function of reaction temperatures.

For all catalysts tested, cracking (C) and hydrogenolysis (H) were the predominant side reactions at high temperatures. The combination of mesoporous silica (MCM-48) and aluminium as support reduced the diffusion limitations for transport and the residence time of the carbocation intermediates at the acidic sites during the isomerization reaction. As a result, the occurrence of cracking and aromatization reactions (A) was limited on the Pt/Al-MCM-48 catalyst. As can be seen in Table 2, the synthesized catalysts form a small aromatization product. However, this amount is not very small in the case of Pt/Zr-MCM-48-Mordenite, suggesting that aromatization is influenced by geometry, acidity, type of acid position and the balance between acid and metal functions. Another important result of our work is the effect of temperature and catalyst type on the research octane number (RON). Equation (3) was used to calculate this parameter [33, 34]:

$$\mathrm{RON} = \sum_{i=1}^{k} y_i \mathrm{RON}_i \tag{3}$$

In this equation, RON_i represents the octane number of the pure component (such as i) and y_i represents the volume fractions of molecule i. The results show that Pt/Al-MCM-48-Mordenite gives a higher RON (RON = 96.5) at 200 °C compared to other catalysts due to the production of molecules with higher RON_i. Deactivation of catalysts by coke is one of the problems in the use of catalysts in industrial processes. To this end, the stability of catalysts for the isomerization of n-heptane at 300 °C after 8 h in operation was investigated. As can be seen from Fig. 6, the performance of the catalysts is almost constant during the course of the reaction and they are not significantly deactivated during this time (TOS = 8 h).

This proves that the catalysts produced have a very stable catalytic performance. However, the decrease is higher for the Pt/Zr-MCM-48-Mordenite and Pt/Al-MCM-48-Mordenite catalysts than for the other catalysts. One reason for this decrease is the rapid formation of coke on the catalyst surfaces. Therefore, coke formation on the catalysts was investigated. Coke combustion is a method to study coke poisoning. Samples tested at 300 °C for 8 h were placed in an oven at 120 °C to lose moisture, then

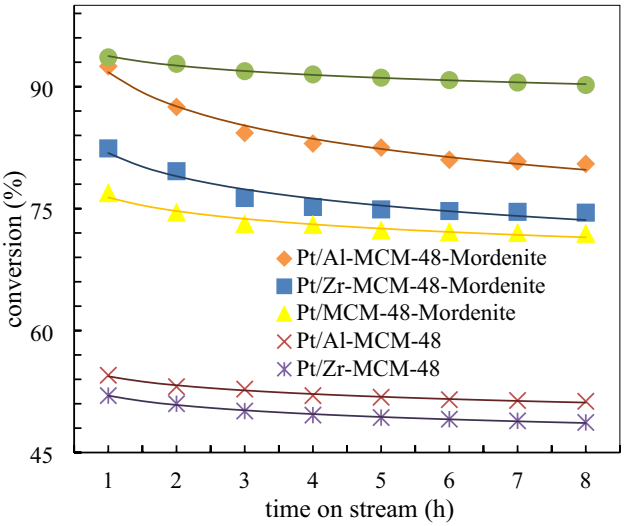

Fig. 6 n-C_7 conversion (%) vs. TOS (h) at 300 °C

weighed and placed in an oven at 300 °C for 1 h. Immediately after cooling, the tested catalyst was weighed again to determine the weight difference. The weight difference is the amount of coke poisoning (Table 2). The small amount of deposited coke indicates the good stability of the prepared catalysts against deactivation during the 8 h operation period. Although the amount of coke (Table 2) is larger for Pt/Al-MCM-48-Mordenite than other catalysts, both the catalytic activity and i-C_7 selectivity are better than others. A TG/DTA analysis was also performed to validate the coke values obtained by this method. The data agree very well with the data obtained by the previous method and do not show any major differences (Table 2).

4 Conclusions

From the results, although Pt/Mordenite catalyst with strongly acidic sites showed high conversion, its products were mainly formed by hydrogenation and cracking. On the other hand, the Pt/Al-MCM-48-Mordenite catalyst showed higher isomerization selectivity. Due to its reasonable acidity, large pores, the appropriate Si/Al ratio and high metal dispersion, it showed the highest yield of multi-branched isomers. The Pt/Al-MCM-48-Mordenite catalyst can be considered as a good candidate for isomerization catalysts. The results show that the hybrid catalysts resulted in high-octane gasoline. Moreover, the stability of the synthesized catalysts is suitable for this isomerization process. However, efforts to improve the results will continue.

Author contributions All authors wrote the main manuscript text, jointly. All authors reviewed the manuscript.

Declarations

Competing interests The authors declare no competing interests.

References

1. V.A. Shkurenok, M.D. Smolikov, S.S. Yablokova, D.I. Kiryanov, A.S. Belyi, E.A. Paukshtis, N.N. Leonteva, T.I. Gulyaeva, A.V. Shilova, V.A. Drozdov, Procedia Eng. **113**, 62–67 (2015)
2. N. Batalha, A. Astafan, J.C. Dos Reis, Y. Pouilloux, C. Bouchy, E. Guillon, L. Pinard, React. Kinet Mech. Catal. **114**, 661–673 (2015)
3. D. Kaucký, B. Wichterlová, J. Dedecek, Z. Sobalik, I. Jakubec, Appl. Catal. A **397**, 82–93 (2011)
4. V.M. Akhmedov, S.H. Al-Khowaiter, Catal. Rev. **49**, 33–139 (2007)
5. S. Lim, Y. Yang, D. Ciuparu, C. Wang, Y. Chen, L. Pfefferle, G.L. Haller, Top. Catal. **34**, 31–40 (2005)
6. M. Selvaraj, P.K. Sinha, K. Lee, I. Ahn, A. Pandurangan, T.G. Lee, Microporous Mesoporous Mater. **78**, 139–149 (2005)
7. Q. Zhang, W. Yang, X. Wang, Y. Wang, T. Shishido, K. Takehira, Microporous Mesoporous Mater. **77**, 223–234 (2005)
8. S. Gontier, A. Tuel, Appl. Catal. A **143**, 125–35 (1996)
9. N. Igarashi, S. Kidani, R. Ahemaito, K. Hashimoto, T. Tatsumi, Microporous Mesoporous Mater. **81**, 97–105 (2005)
10. M.L. Occelli, S. Biz, A. Auroux, Appl. Catal. A **183**, 231–9 (1999)
11. T. Hamoule, M.H. Peyrovi, M. Rashidzadeh, M.R. Toosi, Catal. Commun. **16**, 234–239 (2011)
12. N. Parsafard, A.G. Asil, S. Mirzaei, RSC Adv. **10**, 26034–26051 (2020)
13. W. Tang, H. Zhang, Y. Lu, Y. Yao, S. Lu, J. Porous Mater. **23**, 1489–1493 (2016)
14. J.W. Lee, W.G. Shim, H. Moon, Microporous Mesoporous Mater. **73**, 109–19 (2004)
15. Z. Ghaderi, M.H. Peyrovi, N. Parsafard, BMC Chem. **15**, 1–8 (2021)
16. A. de Lucas, P. Sánchez, F. Dorado, M.J. Ramos, J.L. Valverde, Appl. Catal. A **294**, 215–225 (2005)
17. P. Mäki-Arvela, T.A. Kaka khel, M. Azkaar, S. Engblom, D.Y. Murzin, Catal **8**, 534 (2018)
18. K. Jaroszewska, M. Fedyna, A. Masalska, R. Łużny, J. Trawczyński, Catal **11**, 377 (2021)
19. M. Fedyna, M. Śliwa, K. Jaroszewska, J. Trawczyński, Fuel **280**, 118607 (2020)
20. W. Trisunaryanti, T. Triyono, R. Armunanto, L.P. Hastuti, D.D. Ristiana, R.V. Ginting, Indones J. Chem. **18**, 166–172 (2018)
21. C.E. Webster, R.S. Drago, M.C. Zerner, J. Phys. Chem. B **103**, 1242–1249 (1999)
22. X. Li, R. Prins, J.A. van Bokhoven, J. Catal. **262**, 257–65 (2009)
23. R. Xu, W. Pang, J. Yu, Q. Huo, J. Chen, *Chemistry of Zeolites and Related Porous Materials* (Wiley-VCH Verlag GmbH & Co. KGaA, 2010), pp. 1–13, 19–47 and 176
24. M. Anbia, K. Kargosha, S. Khoshbooei, Chem. Eng. Res. Des. **93**, 779–788 (2015)
25. R. Peng, C.M. Wu, J. Baltrusaitis, N.M. Dimitrijevic, T. Rajh, R.T. Koodali, Int. J. Hydrog. Energy **41**, 4106–4119 (2016)
26. H.M. Aly, M.E. Moustafa, E.A. Abdelrahman, Adv. Powder Technol. **23**, 757–60 (2012)
27. M.L. Mignoni, D.I. Petkowicz, N.R. Machado, S.B. Pergher, Appl. Clay Sci. **41**, 99–104 (2008)
28. J. Wang, W. Zhang, Y. Suo, Y. Wang, J. Porous Mater. **25**, 1317–1324 (2018)
29. L.Y. Chen, Y.Q. Ni, J.L. Zang, L.W. Lin, X.H. Luo, S. Cheng, J. Catal. **145**, 132–140 (1994)
30. H. Yunfeng, W. Xiangsheng, G. Xinwen, L. Silue, H. Sheng, S. Haibo, B. Liang, Catal. Lett. **100**, 59–65 (2005)
31. Y. Bi, G. Xia, W. Huang, H. Nie, RSC Adv. **5**, 99201–99206 (2015)
32. G. Talebi, M. Sohrabi, S.J. Royaee, R.L. Keiski, M.H. Imamverdizadeh, H J. Ind. Eng. Chem. **14**, 614–621 (2008)
33. Z. Ghaderi, M.H. Peyrovi, N. Parsafard, J Iran. Chem Soc. **15**, 1–7 (2022)
34. Z. Ghaderi, M.H. Peyrovi, N. Parsafard, React. Kinet Mech. Catal. **21**, 1–3 (2022)